[PS]Petroleum Expulsion and Formation of Porosity in Kerogen*

Alton Brown[1]

Search and Discovery Article #42388 (2019)**
Posted July 22, 2019

*Adapted from poster presentation given at AAPG 2019 Annual Convention & Exhibition, San Antonio, Texas, May 19-22, 2019
 DOI:10.1306/42388Brown2019

[1]Consultant, Richardson, TX, United States (altonabrown@yahoo.com)

Abstract

This study evaluates the magnitude and distribution of petroleum pressure within a source rock, drive mechanism for expulsion, and kerogen volume changes during transformation. Together, these concepts explain why kerogen is more porous in some source rocks than in others. Petroleum pressures within a sheet-shaped source rock equilibrate rapidly (<1 My), and pressure distribution can be modeled as a pseudo-steady process. The vertical distribution of petroleum excess pressure within the sheet acquires a warped hyperbolic shape. Generation causes a symmetric petroleum excess pressure distribution that is zero at the top and base of the sheet and highest in the middle. This petroleum pressure is superimposed on a capillary pressure gradient controlled by water-petroleum density difference and fluid pressures at the top and base of the sheet of source rock. The capillary pressure gradient controls the direction of expulsion more than the magnitude of excess pressure. Petroleum excess pressure increases with increasing petroleum generation rate, increasing source-rock thickness, and decreasing petroleum mobility. Modeled excess pressure does not exceed a few hundred psi except where source rocks are very thick (hundreds of m), generation rates are very high, or petroleum mobility is low (picodarcy/centipoise). For typical thin source rocks, excess pressures are on the order of a few psi. The excess pressure driving expulsion is too low to significantly reduce source-rock effective stresses during generation. Density of oil-prone kerogen increases with decreasing hydrogen index and hydrogen/carbon ratio; therefore, kerogen volume changes with transformation can be modeled using initial hydrogen index and transformation ratio. The kerogen shrinks as its mass is converted to petroleum and its hydrogen content decreases. Where kerogen forms part of the framework supporting overburden stress, the source rock consolidates as fast as the kerogen shrinks (compaction equilibrium). The source rock thins during transformation, but generation creates negligible porosity in kerogen. Porosity forms in kerogen only where effective stress remains low during and after generation. For example, the mechanical strength of rigid bodies shelters adjacent kerogen from high effective stresses. Kerogen porosity is more likely to form and be preserved in source rocks rich in silt-sized and coarser rigid grains than in clay-rich source rocks.

References Cited

Aguilera, R., 2016, Shale gas reservoirs: Theoretical, practical and research issues: Petroleum Research, v. 1, p. 10-26.

Brown, A.A., 2002, Petroleum Charge Analysis of the Southern San Joaquin Basin, California: Implications for Future Exploration: 2002 AAPG National Meeting, March 2002.

Byrnes, A.P, S. Zhang, L. Canter, and M.D. Sonnenfeld, 2018, Two-phase and three-phase relative permeability of unconventional Niobrara chalk using integrated core and 3D image rock physics: Denver Well logging society presentation in Jan 2018, downloaded from http://dwls.spwla.org/2018-01-16%20DWLS%20 on 25 April 2019.

Carslaw, H.S., and J.C. Jaeger, 1959, Conduction of heat in solids, 2d. ed.: Clarendon Press, Oxford, 510 p.

Cooles, G.P., A. Mackenzie, and T.M. Quigley, 1986, Calculation of petroleum masses generated and expelled from source rocks: Organic geochemistry, v. 10/1-3, p. 235-245.

Di Primio, R., and B. Horsfield, B., 2006, From petroleum-type organofacies to hydrocarbon phase prediction: AAPG bulletin, v. 90/7, p. 1031-1058.

Eslinger, E., and R.V. Everett, 2009, Petrophysics in generic gas shales with examples from the Haynesville: Haynesville shale gas technology symposium, Society of Petroleum Engineers – Dallas Section, September 15, 2009.

Franklin, R.E., 1948, A note on the true density, chemical composition, and structure of coals and carbonized coals: Fuel, 1948, v. 27, p. 46–49.

Gan, H., S.P. Nandi, and P.L. Walker Jr., 1972, Nature of the porosity in American coals. Fuel, v. 51/4, p. 272-277.

Gorshkov, A.M., L.K. Kudryashova, and O.S. Lee-Van-Khe, 2016, Petrophysical rock properties of the Bazhenov Formation of the South-Eastern part of Kaymysovsky Vault (Tomsk Region): IOP Conference Series: Earth and Environmental Science, v. 43, p. 012010. Downloaded from https://iopscience.iop.org/article/10.1088/1755-1315/43/1/012010/pdf on 25 April 2019.

Han, Z., M.A. Kruge, J.C. Crelling, and B.A. Stankiewicz, 1995, Organic geochemical characterization of the density fractions of a Permian torbanite: Organic geochemistry, v. 22/1, p. 39-50.

Loucks, R.G., R.M. Reed, S. Ruppel, and U. Hammes, 2012, Spectrum of pore types and networks in mudrocks and a descriptive classification for matrix-related mudrock pores: AAPG Bulletin, v. 96/6, p. 1071-1098.

Mackenzie, A.S., I. Price, D. Leythaeuser, P. Muller, M. Radke, and R.G. Schaefer, 1987, The expulsion of petroleum from Kimmeridge Clay source-rocks in the area of the Brae oilfield, UK continental shelf: Petroleum geology of north west Europe, v. 2, p. 865-877.

Matthews, C.S. and D.G. Russell, 1967, Pressure buildup and flow tests in wells: H.L. Doherty series, Monograph 1, Society of Petroleum Engineers,

Richardson, TX, 167 p.

Milliken, K.L., W.L. Esch, R.M. Reed, and T-W. Zhang, 2012, Grain assemblages and strong diagenetic overprinting in siliceous mudrocks, Barnett Shale (Mississippian), Fort Worth Basin, Texas: AAPG Bulletin, v. 96/8, p. 1553–1578.

Nip, M., J.W. De Leeuw, P.A. Schenck, W. Windig, H.L.C. Meuzelaar and J.C. Crelling, 1989, A flash pyrolysis and petrographic study of cutinite from the Indiana paper coal: Geochimica et Cosmochimica Acta, v. 53/3, p. 671-683.

Okiongbo, K. S, 2011, Bulk volume reduction of the Kimmeridge Clay Formation, North Sea (UK) due to compaction, petroleum generation, and expulsion: Research Journal of Applied Sciences, Engineering, and Technology, v. 3/2, p. 132-139.

Okiongbo, K.S., A.C. Aplin, and S.R. Larter, 2005, Changes in type II kerogen density as a function of maturity: Evidence from the Kimmeridge Clay Formation: Energy & fuels, v. 19/6, p. 2495-2499.

Osborne, M.J. and R.E. Swarbrick, 1997, Mechanisms for generating overpressure in sedimentary basins: a reevaluation: AAPG Bulletin, v. 81/6, p. 1023-1041.

Pepper, A.S. and P.J. Corvi, 1995, Simple kinetic models of petroleum formation. Part III: modelling an open system: Marine and Petroleum Geology, v. 12/4, p. 417-452.

Robl, T.L., D.N. Taulbee, L.S. Barron, and W.C. Jones, 1987, Petrologic chemistry of a Devonian type II kerogen: Energy & fuels, v. 1/6, p. 507-513.

Stolz, D.J., 2014, Reservoir Character of the Avalon Shale (Bone Spring Formation) of the Delaware Basin, West Texas and Southeast New Mexico: Effect of Carbonate-rich Sediment Gravity Flows: MS thesis, University of Kansas, 165 p.

Sweeney, J.J. and A.K. Burnham, 1990, Evaluation of a simple model of vitrinite reflectance based on chemical kinetics: AAPG Bulletin, v. 74/10, p. 1559-1570.

Walls, J.D., A. Morcote, T. Hintzman, M. Everts, 2016, Comparative core analysis from a Wolfcamp formation well; a case study: paper SCA2016-044, International Symposium of the Society of Core Analysts held in Snow Mass, Colorado, USA, 21-26 August 2016, 6 p.

Walls, J.D., and S.W. Sinclair, 2011, Eagle Ford shale reservoir properties from digital rock physics: First Break, v. 29/6, p. 97-101.

Petroleum Expulsion and Formation of Porosity in Kerogen

Brown, Alton A., Consultant, altonabrown@yahoo.com

Abstract

This study evaluates the magnitude and distribution of petroleum pressure within a source rock, drive mechanism for expulsion, and kerogen volume changes during transformation. Together, these concepts explain why kerogen is more porous in some source rocks than in others.

Petroleum pressures within a sheet-shaped source rock equilibrate rapidly (<1 My), and pressure distribution can be modeled as a pseudo-steady process. The vertical distribution of petroleum excess pressure within the sheet acquires a warped hyperbolic shape. Generation causes a symmetric petroleum excess pressure distribution that is zero at the top and base of the sheet and highest in the middle. This petroleum pressure is superimposed on a capillary pressure gradient controlled by water-petroleum density difference and fluid pressures at the top and base of the sheet of source rock. The capillary pressure gradient controls the direction of expulsion more than the magnitude of excess pressure.

Petroleum excess pressure increases with increasing petroleum generation rate, increasing source-rock thickness, and decreasing petroleum mobility. Modeled excess pressure does not exceed a few hundred psi except where source rocks are very thick (hundreds of m), generation rates are very high, or petroleum mobility is low (picodarcy/centipoise). For typical thin source rocks, excess pressures are on the order of a few psi. The excess pressure driving expulsion is too low to significantly reduce source-rock effective stresses during generation.

Density of oil-prone kerogen increases with decreasing hydrogen index and hydrogen/carbon ratio; therefore, kerogen volume changes with transformation can be modeled using initial hydrogen index and transformation ratio. The kerogen shrinks as its mass is converted to petroleum and its hydrogen content decreases. Where kerogen forms part of the framework supporting overburden stress, the source rock consolidates as fast as the kerogen shrinks (compaction equilibrium). The source rock thins during transformation, but generation creates negligible porosity in kerogen.

Organic porosity is preserved only where effective stress remains low during and after generation. Generation pressure cannot do this. However, rigid components in the rock (grains) can shelter kerogen from high effective stresses. Therefore, kerogen porosity is more likely to be preserved where rigid grains comprise most of the source rock.

Introduction

Petroleum generated in a source rock must leave the source rock to charge conventional accumulations. This process is referred to as expulsion or primary migration. Expulsion implies petroleum migration within the source rock, because petroleum generated within the source rock must reach its edge before it can be expelled. In some source rocks, unexpelled petroleum forms economic, but "unconventional" petroleum accumulations. The volume of petroleum in these accumulations depends on how much petroleum was <u>not</u> expelled. Understanding expulsion is important, because the process of expulsion separates two distinct pathways of petroleum evolution, with expelled petroleum forming conventional and tight-reservoir accumulations, and unexpelled petroleum forming unconventional source-rock accumulations.

Do economic source-rock oil and gas accumulations have less expulsion? Are economic source-rock oil and gas accumulations limited to settings with significantly lower expulsion efficiency? How does the occurrence of organic porosity (porosity developed within the kerogen) affect the expulsion efficiency?

To address these issues, expulsion relationships to source richness and petroleum transformation are first reviewed and generalized. Literature data indicate high expulsion efficiency in rich source rocks, even where they economically produce oil and gas. Fluid flow through source rocks is then analytically modeled to generalize the expulsion problem. Pressure needed to expel petroleum is modeled as a function of source rock thickness, permeability, and volumetric petroleum generation rate. Pressure generation by kerogen-petroleum volume changes are compared to those from compaction. Implications of the relatively low modeled excess pressures on formation and preservation of organic porosity are then tested by comparing model trends to storage observed in source rocks.

Expulsion Efficiency

Expulsion efficiency can be estimated by mass balance using geochemical data, especially programmed temperature pyrolysis data (Cooles et al. 1986; McKenzie et al. 1987; Pepper and Corvi 1995). Generated petroleum is estimated from the S_2 pyrolysis peak and transformation ratio (TR). Petroleum resident in the sample is estimated from the S_1 pyrolysis peak with suitable corrections for volatilized petroleum and (for gas window samples) sorbed gas and gas stored in porosity. The expulsion efficiency, (EE) is the expelled petroleum (generated petroleum minus the corrected resident petroleum) divided by the generated petroleum.

Figure 1-1 summarizes general EE trends with TR and initial source quality expressed as initial generation potential, S_2^o. Essentially all source rocks with high S_2^o and TR > 0.3 have high EE (typically greater than 0.7). As S_2^o decreases, EE decreases and threshold TR for expulsion increases. Figure 1-2 shows amount of petroleum expelled divided by the total potential generation as a function of TR for San Joaquin basin Miocene-aged samples (Brown 2002). At low TR, expulsion is slower than generation and HC content of samples increases. However, at TR > 0.2, the expelled petroleum trend is parallel to the generation trend, indicating an expulsion rate approximately equal to generation rate. This "steady" expulsion develops after samples have been saturated with about 17% of the generated petroleum (83% of petroleum expelled).

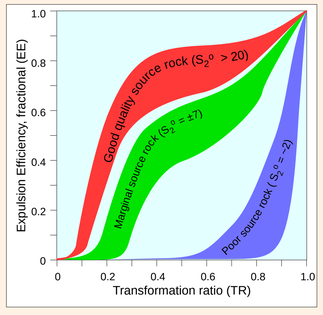

Figure 1-1. Summary of expulsion efficiency as a function of TR and initial source richness as expressed by S_2^o. EE increases with TR and source richness. Summarized from many literature and proprietary studies.

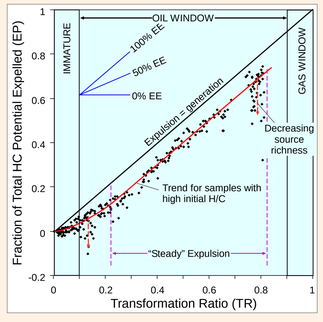

Figure 1-2. Petroleum expulsion from Miocene-aged San Joaquin basin samples as a function of TR. Expulsion trend is parallel to the generation trend for rich samples, indicating steady expulsion. Samples below the data trend have lower S_2^o and therefore lower EE. Modified from Brown (2002).

Kerogen and Petroleum Density

Kerogen and petroleum density estimates are needed to evaluate porosity storage in source rocks and volume changes during generation. The density of kerogen with low oxygen content has a strong correlation to its hydrogen content regardless of rank (Franklin, 1948; Figure 1-3). For this study, H/C in literature data was converted to hydrogen index, thus allowing calculation of kerogen density in any sample with a hydrogen index estimate. Oxygen-poor kerogen density is linearly correlated to HI down to about 25 mg HC/g C. At lower hydrogen content, kerogen density increases much more steeply. These data were fit to the following relationship: If HI > 25, $\rho = 1.361 - 0.00044HI$; if HI < 25, $\rho = 1.75 - 0.016HI$, where kerogen density (ρ) is in g/cm^3 and hydrogen index (HI) is in mg HC/g rk.

Generated petroleum composition changes as the source rock matures (Figure 1-4). Pressure and temperature are sufficiently high during natural petroleum generation for the petroleum to form a single phase at all maturation levels. Pressure and temperature affect fluid densities. No pressure - temperature conditions are specified in this work. Therefore, an empirical, generalized relationship between petroleum density and TR was modeled for this study: $\rho_{oil} = 0.8 - 0.28*TR$ where HI > 25; if HI < 25, $\rho_{gas} = 0.2$. Modeled kerogen and petroleum density trends with TR differ for different initial HI (HI^o, Figure 1-5).

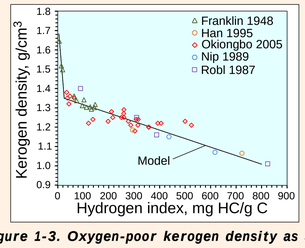

Figure 1-3. Oxygen-poor kerogen density as a function of hydrogen index. Some data were converted from elemental H/C ratios to HI. Black line is kerogen density model used for this study.

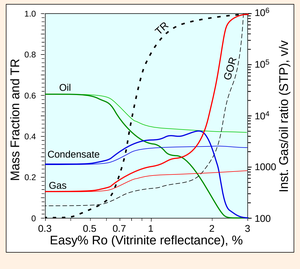

Figure 1-4. Changes of oil, gas, and condensate fractions with vitrinite reflectance using Woodford compositional kinetics (Di Primio and Horsfield 2006) Easy%Ro model (Sweeney and Burnham 1990) and 2°C/My heating rate. Cumulative fractions (thin lines) include all generation up to that maturation; instantaneous fractions (heavy lines) are fractions generated at that maturation. TR (heavy dashed line) and GOR (light dashed line) are also plotted. No oil cracking is modeled. Gas is the sum of methane, ethane, and propane. Condensate is the sum of all butanes to hexanes. Oil is the sum of all heavier components.

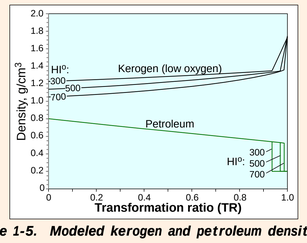

Figure 1-5. Modeled kerogen and petroleum density as a function of TR and initial HI (HI^o).

Analytical Expulsion Models

The expulsion problem is part of a general class of combined flow and generation problems that includes heat flow, diffusion, and volumetric flow. Because source rocks are stratigraphic bodies with a generalized slab-shaped geometry, the geometry to be modeled is that of an infinite slab where transport is one dimensional normal to the surfaces of the slab. The problem of combined generation and flow from infinite slabs has been addressed mathematically in heat-flow problems (e.g., Carslaw and Jaeger 1959). Heat flow solutions can be readily adapted to volumetric flow problems by modifying the flow constants (Matthews and Russell 1967). Volumetric flow is controlled by the slab half-thickness, generation rate, and flow parameters. Solutions for volumetric flow are the pressure distribution within the slab and the flow rate at positions within the slab and at the edges of the slab.

Published analytical solutions require simplified source rock properties and boundary conditions. Source rock half-thickness is uniform and constant. Generation rate has to be a simple function of position within the slab and of time. The simplest case is uniform (same generation rate at all positions in the source rock) and constant (generation rate not a function of time). Solutions addressed here have constant pressure boundary conditions (pressures at each slab surface is kept constant).

Temperatures within a heat-generating slab under these boundary conditions is presented in Carslaw and Jaeger (1959, eq. 3.14.7). Converting to fluid fluid flow gives pressure (p) distribution within the slab as a function of time (t) and position (x):

$$p = \frac{AL^2}{2K}\left\{1 - \frac{x^2}{L^2} - \frac{32}{\pi^3}\sum_{n=0}^{\infty}\frac{(-1)^n}{(2n+1)^3}\cos\frac{(2n+1)\pi x}{2L}\exp\left(\frac{-k(2n+1)^2\pi^2 t}{4L^2}\right)\right\} \quad (1)$$

where K is the steady flow parameter which for volumetric flow is the mobility (permeability divided by viscosity). A is volumetric generation rate. L is half-thickness of the slab, and x is the position relative to the center of the slab where x = 0 at the center of the slab and x = 1 at the top edge of the slab. The transient flow parameter (k) is called the hydraulic diffusivity for fluid flow problems (Matthews and Russell 1967).

The expulsion rate is flow per unit area (q) across the edge of the slab. Expulsion is the negative of the pressure gradient at the slab edge multiplied by the steady flow constant K. Pressure gradient is determined by differentiating equation 1 at +1 and -1. The rate of expulsion away from the center of the slab is:

$$q = AL\left\{1 - \frac{8}{\pi^2}\sum_{n=0}^{\infty}\frac{\exp(-k(2n+1)^2\pi^2/4)}{(2n+1)^2}\right\} \quad (2)$$

Transition from Transient to Steady Flow

Steady flow develops where flow from the slab balances the generation within the slab. Under steady conditions, pressure is no longer a function of time. Equations 1 and 2 then simplify to:

$$p = \frac{A}{2K}(L^2 - x^2) \quad \text{(3a) and} \qquad q = AL \quad \text{(3b)}$$

The transition to steady flow can be determined by evaluating the dimensionless parameter kt/L^2. The steady model can be used where kt/L^2 is sufficiently large. For 90% of steady pressure, kt/L^2 is 0.946; for 99%, kt/L^2 is 1.88; for 99.9%, kt/L^2 is 2.81. Using the steady model not only speeds calculations, it allows modeling of much more complex settings where generation rate, permeability, viscosity, source thickness, etc. change as sediment is buried. Where pressure equilibration is much faster than changes in these properties, conditions can be described as "pseudo-steady" and the transient problem can be solved by a series of steady models with varying generation rate, permeability, thickness, etc. (This approach is used for heat flow in most geohistory models, for example).

For discussion purposes, pressure equilibration to 99% of steady pressure in the center of the slab (x=0) within a million years (3.15E13 s) is sufficiently fast to use pseudo-steady models to estimate pressures during generation. By this definition, steady conditions develop where kt/L^2 is 1.88. The maximum value of k and its constituents can be estimating by solving for k using the kt/L^2 of 1.88.

For flow of a low compressibility fluid such as oil, k is the mobility divided by fractional porosity and fluid compressibility (Matthews and Russell 1967). Assuming reservoir oil viscosity is 0.001 pa-s (1 cp), fractional porosity of 0.1, and compressibility is 1.45E-9/Pa (about 1E-5/psi), the permeability above which steady pressures develop within a million years as a function of the assumed source rock half-thickness are shown on Figure 1-6. Steady flow develops at very low permeability under these conditions. For example, oil permeability greater than 0.1 nD develops steady flow in a source rock with 107 m or less half-thickness in a million years. With 0.001 nD oil permeability, steady conditions develop in a million years where half-thickness is 11 m (Figure 1-6).

For flow of an ideal gas, k is mobility divided by twice the porosity (Matthews and Russell 1967). Assuming 0.1 fractional porosity and a viscosity of 2E-5 pa-s (0.02 cp), the permeability above which steady conditions develop within a million years are much higher than those of oil due to the greater compressibility of gas (Figure 1-6). For 100 m half-thickness, steady flow develops where gas-phase permeability is greater than 2.4 mD. For 10 m half-thickness, permeability must be greater than 0.024 mD. These permeabilities are much higher than those reported for source-rock shales (see sheet 2); therefore, gas generation and expulsion has to be modeled by the transient equation. Fortunately, the much lower viscosity of gas results in much lower excess pressure development in a source rock. Also, the steady gas pressures are greater than transient gas pressures; therefore use of the steady model overestimates rather than underestimates gas pressure.

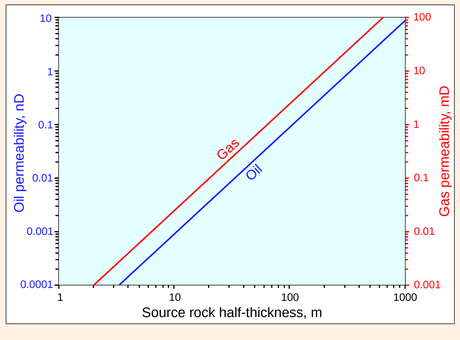

Figure 1-6. Petroleum permeability above which steady pressure develops in a source rock in a million years plotted as a function of half-thickness of the source rock. For oil (blue line), steady conditions develop at very low permeability, in the picodarcy to nanodarcy range. Gases require permeability in the microdarcy to millidarcy range to develop steady flow within a million years.

PETROLEUM EXPULSION AND FORMATION OF POROSITY IN KEROGEN

Brown, Alton A., Consultant, altonabrown@yahoo.com

Analytical Solutions to Steady Expulsion

Base Case: No Buoyancy or Capillary Pressure Effects

Assume a homogeneous, sheet-shaped source rock generating petroleum at a uniform and constant volumetric rate *A*. The source rock has a uniform petroleum permeability *k*, and it is surrounded by a permeable sandstone saturated with petroleum with the same density as that generated in the source rock. Generated petroleum has a constant viscosity μ. Petroleum expelled into surrounding rock migrates away as fast as it is expelled so that excess petroleum pressure at the edges of the source rock is zero. (Excess petroleum pressure is the petroleum pressure minus the pressure caused by the weight of the petroleum). Flow is steady; that is, petroleum is expelled from the source rock as fast as it is generated and pressure does not change with time in the source rock or in adjacent beds. Because surrounding fluid is petroleum with the same density as generated petroleum, buoyancy and capillary pressure effects can be ignored.

Petroleum generated from the entire source volume is expelled from its edges. Therefore, petroleum volume crossing each plane parallel to the edges must increase from zero at the center (the divergence) to a maximum value at the edge of the source rock. Flow is proportional to excess pressure gradient; therefore, the excess pressure gradient steepens to accommodate the greater fluid flow as it approaches the edge of the source rock. These conditions cause a hyperbolic excess pressure distribution with highest excess pressure at the divergence (Figure 2-1). Excess pressure (*p*) is described by the following relationship:

$$p = \frac{A(L^2 - x^2)}{2K} \qquad \text{(Eq. 3a)}$$

where *L* is the half-thickness of the source rock, *x* is position relative to the center of the source rock, and *K* is the mobility (*k*/μ, permeability/viscosity). Equation 3a is modified from Carslaw and Jaeger (1959, eq. 3.14-2). Pressure described by equation 3a will be referred to as the dynamic pressure.

Maximum dynamic pressure is at the center of the source rock (*x* = 0). Maximum excess petroleum pressure increases with generation rate and thickness squared and decreases with increasing mobility. The volume of source rock above the divergence equals that below the divergence; therefore, equal amounts of petroleum are expelled from the upper and lower surface of the source rock.

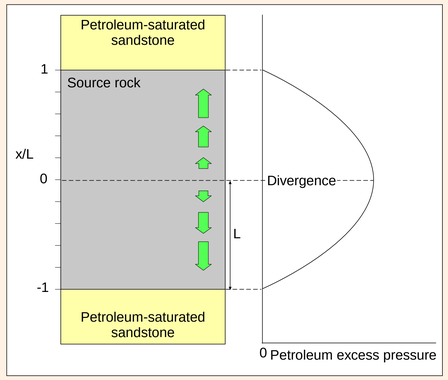

Figure 2-1. Schematic pressure distribution in a source rock with steady generation and expulsion into an oil-saturated permeable medium above and below the source rock. Volumetric flow rate of petroleum (green arrows) increases towards the edges of the source rock to accommodate cumulative generation from center of the source rock. The divergence is the highest excess pressure in the source rock, and it separates flow directions.

Effect of Buoyancy

Assume now that surrounding beds are saturated with water rather than petroleum. This introduces buoyancy effects. Boundary conditions for expulsion is that the petroleum pressure equals the water pressure at both upper and lower boundaries (if not, petroleum cannot displace the water and cannot be expelled from the source). Water is denser than petroleum; therefore, petroleum at the base of the source rock must have a higher pressure than that at the top of the source rock to be expelled. This pressure is $2Lg(\rho_w - \rho_h)$, where ρ is the fluid density, *g* is the pressure gradient of water, and subscripts *w* and *h* refer to water and petroleum, respectively.

Buoyancy effects on pressure are superimposed on (added to) the dynamic pressure. Maximum petroleum excess pressure (divergence) is shifted below the center of the source rock (Figure 2-2). More source volume is above the divergence than below the divergence; therefore, more petroleum is expelled through the upper source-rock boundary than the lower source-rock boundary. Where dynamic pressure is sufficiently low, all petroleum is expelled upwards. The magnitude of the buoyancy effect is relatively small. Assuming a fluid density difference of 0.8 g/cc (for gas-water) and a thickness of 100 m (L = 50 m), the pressure at the base of the source rock is about 0.78 MPa (114 psi) higher than that at the top of the source rock.

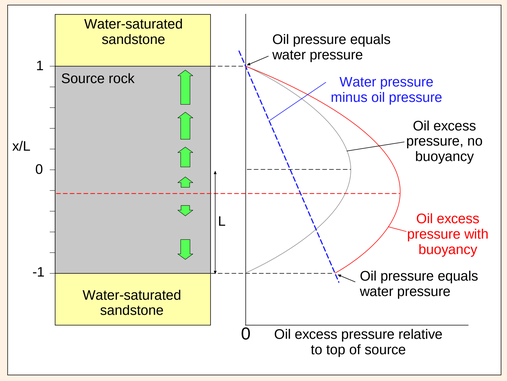

Figure 2-2. Schematic pressure distribution in a source rock with steady generation and buoyancy effects on boundary pressures (water-saturated sandstone above and below the source). Pressure is higher on the lower boundary due to the weight of the water. This increases the maximum excess pressure in the source rock and shifts the divergence down so that more petroleum is expelled from the top of the source rock.

Boundary Lithology Effects

Petroleum source rocks are oil-wet systems and capillary effects on migration within the source rock are small. However, capillary effects have to be considered where petroleum is expelled into water-wet rocks. Different rock types have different threshold capillary pressures. For petroleum to be expelled from the source rock, the capillary pressure at the edge of the source rock must exceed the water pressure plus threshold capillary pressure (P_t) of the rock surrounding the source rock. (Capillary pressure is petroleum pressure minus water pressure at the same position in the rock). Therefore, boundary condition for steady expulsion is petroleum pressure equal to the sum of water pressure plus threshold pressure at the edges of the source rock. The petroleum pressure within the source rock is the pressure interpolated between the two boundary pressures superimposed on (added to) the dynamic pressure (Figure 2-3).

For water-wet matrix pore systems, capillary threshold pressure increases as permeability decreases. Threshold pressure of petroleum-water systems can be roughly approximated by dividing the mercury injection capillary pressure (MICP) by 10. Threshold pressures of fine-grained rocks can be relatively high. For example, a water-wet shale with 8000 Hg psi P_t has about 800 psi oil-water P_t. Petroleum pressure has to be about 800 psi (5.5 MPa) greater than water pressure at that boundary for petroleum to be expelled.

Where a source rock is surrounded by different lithologies, most petroleum will be expelled in the direction of lowest threshold pressure, because the threshold pressure difference is typically much larger than pressure differences from buoyancy. Water-wet shale over source rock over sandstone will lead to predominantly downwards expulsion; sandstone over source rock over water-wet shale will result in almost complete upwards petroleum expulsion.

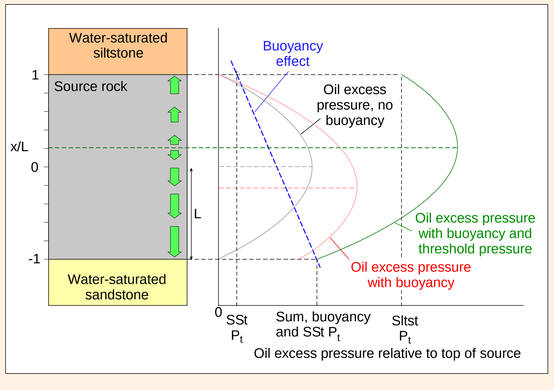

Figure 2-3. Schematic pressure distribution in a source rock with steady generation, buoyancy, and lithology effects on boundary pressures. P_t of surrounding lithologies increase maximum petroleum excess pressure in the source rock and controls direction of petroleum expulsion. In this example, P_t of the overlying siltstone is higher than that of the sandstone below the source rock. Therefore, most expulsion is through the lower source edge rather than the upper source edge.

Source Rock Properties

Permeability

Matrix permeability of organic-rich mudrocks are available for a number of gas- and oil-productive source rocks as well as a few non-productive source rocks (Figure 2-4). Data shown on this figure are a mix of GRI analyses with gas-saturated porosity and gas-phase permeability, digital rock physics measurements of total porosity and modeled permeability, and other methods. In general, porosity and permeability estimates from digital rock physics roughly match GRI estimates of cleaned samples (Walls and Sinclair 2011). However, measurements are unstressed and Klinkenberg corrections may be incomplete. For these reasons, the permeability data plotted here demonstrate the expected range of permeability in source rocks of different average porosities rather than precise values.

Based on these and other data, average permeability in most gas- and oil-productive source rocks is on the order of nanodarcys (nD) to hundreds of nD. The two examples of non-productive source rocks (Kimmeridge and Bazhenov) show oil-window permeabilities in the range of 0.01 to 1 nD.

Viscosity

Liquid petroleum viscosity decreases as gas content increases with maturity. At pressures and temperatures near peak generation, viscosity is probably close to 1 cp. Gas viscosity is much lower and more sensitive to temperature. At gas generation temperatures, gas viscosity is probably close to 0.02 cp. Viscosity of fluids near the transition of oil to gas are uncertain, but peak generation rates occur during liquids generation. Both gas and oil viscosity changes have much less variation and uncertainty than permeability estimates. Viscosity of petroleum in the oil window will be modeled as 0.001 Pa-s (1 cp). Viscosity in the gas window will be modeled as 2E-5 Pa-s (0.02 cp). The effects of permeability are better illustrated by a step change in viscosity.

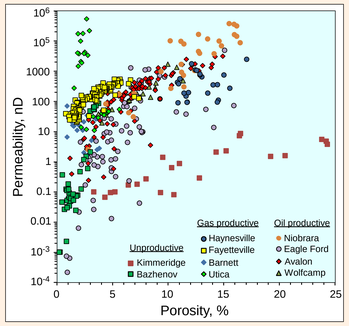

Figure 2-4. Compilation of literature porosity and permeability measurements for source rocks and productive shales. Sources: Kimmeridge: Okiongbo (2011); Bazhenov: Gorshkov et al. (2016); Haynesville: Eslinger and Everett (2009); Fayetteville: Aguilera (2016); Barnett: Milliken et al. (2012); Utica: Aguilera (2016); Niobrara: Byrnes et al. (2018); Eagle Ford: Walls and Sinclair (2011); Avalon: Stolz (2014); Wolfcamp: Walls et al. (2016).

Volumetric Petroleum Generation Rates

Geohistory and kinetics programs report generation rates as mass rates: mass petroleum/mass rock/time. Generation rate increases with heating rate and initial source richness for any given kinetics. This analytical expulsion model uses volumetric rates: volume petroleum/volume porous rock/time. Multiply the mass rate by the ratio of bulk rock to petroleum density to get the volumetric rate.

Woodford kinetics (Di Primio and Horsfield 2006) were used to calculate mass generation rates. Bulk density depends on mineral grain density, kerogen density and abundance, and assumed porosity. Mineral grain density was assumed to be constant at 2.7 g/cc. Modeled petroleum density and kerogen density are shown on Figure 1-5 (Sheet 1). Porosity is assumed constant at 5% for mass to volumetric generation rate conversion. Porosity and minor grain mineral density variations have minor effects on the volumetric generation rate.

Modeled volumetric generation rate shows two peaks, one at peak oil generation and the second during early gas generation (Figure 2-5). The gas peak is caused by the abrupt decrease in gas density, which increases the volumetric generation rate relative to mass rate. For kinetics similar to Woodford, peak generation rate in the oil window is about 3 times higher than the gas peak for all heating rates. (Figure 2-6).

The maximum volumetric generation rates estimated from literature and proprietary geohistory models for various source rocks is plotted against the initial generation potential (Figure 2-7). Maximum volumetric generation rates in example source rocks vary from about 0.0008/My to 0.06/My.

Assuming a thermal gradient of 30° C/km, 1° C/My to 50° C/My heating rates correspond to 33 m/My (110 ft/My) to 1666 m/My (5500 ft/My) burial rates, respectively. Heating rate of 50° C/My is probably close to the maximum heating rate that can be expected by burial in sedimentary basins. Most source rocks probably see heating rates slower than 20° C/My during peak oil generation.

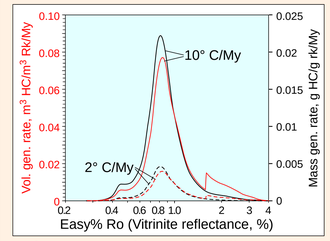

Figure 2-5. Volumetric (red) and mass (black) generation rates for Woodford kerogen at heating rates of 2° C (dashed lines) and 10° C (solid lines). Volumetric rates have two peaks due to different oil and gas densities. Heating rates correspond, respectively, to 66 and 333 m/My burial rates where thermal gradient is 30° C/km. Based on Woodford Kinetics.

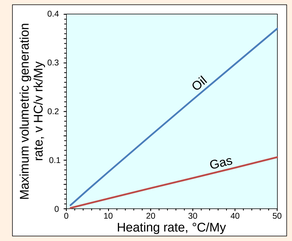

Figure 2-6. Maximum volumetric generation rate for oil (blue) and gas (red) given Woodford kinetics and the initial generation potential (S_2^o) of 93.53 mg HC/g rk reported for the Woodford sample.

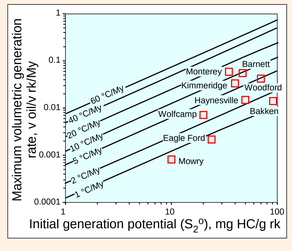

Figure 2-7. Maximum volumetric generation rate for oil as a function of initial generation potential and heating rate (lines). Red squares are estimated average S_2^o and heating rates at peak oil generation for example source rocks discussed later. Maximum volumetric generation rates of example source rocks fall between 0.0008/My and 0.06/My.

Source-Rock Half-Thickness

The thickness of interest is that of the source-rock facies, not of the formation. For example:

- The Bakken Formation has two black shale units that are the source of Bakken oil. Total Bakken thickness includes the middle dolomitic siltstone which is not a source. The half-thickness of the individual upper and lower black shale members should be used for expulsion modeling.
- The Wolfcamp Formation is predominantly shale with many relatively thin intervals with high petroleum source potential. The thickness of the units with source potential should be modeled, not the total Wolfcamp thickness. Total Niobrara, Eagle Ford, and Kimmeridge Formations are also significantly thicker than their source facies.

Source rocks thin to zero at their depositional limits. Maximum half-thicknesses of source-rock facies are typically in the range from about a meter to about one hundred of meters. Because source rocks have a wide range of thickness, half-thicknesses is plotted as the variable against various controls on excess pressure development.

PETROLEUM EXPULSION AND FORMATION OF POROSITY IN KEROGEN

Brown, Alton A., Consultant, altonabrown@yahoo.com

Model Results

Approach

The goal is to determine the highest dynamic excess pressure that develops in a source rock with specified properties and generation rates as a function of generation rate, permeability, and thickness. Dynamic pressure distribution within a source rock is hyperbolic and scaled to the pressure at the center of the bed, which is the highest excess pressure. Excess pressure is highest under steady generation and expulsion. Therefore, steady dynamic pressure at the center of the bed will be calculated using the steady equation (3a) with x = 0. In the following figures, pressures are the dynamic excess pressures in the center of the source rock.

Maximum volumetric generation rates develop during peak oil generation (see Sheet 2). Oil viscosity is higher than gas viscosity. The combination of higher generation rate and higher viscosity results in oil excess pressures much greater than gas excess pressures in otherwise equal settings.

Range of source rock properties are discussed on Sheet 2. Dynamic petroleum pressures are plotted as a function of source-rock half thickness, because the thickness varies the most within and between source rocks. Two other properties are considered, the volumetric generation rate and the permeability of the source rock. A volumetric generation rate of 0.02/My is used to determine effects of permeability on excess dynamic pressure. A permeability of 0.1 nD is used to evaluate the effect of volumetric generation rate on dynamic pressure.

Effects of Permeability

Dynamic pressure in the center of an oil-generating source rock is plotted as a function of thickness and permeability for a generation rate of 0.02/My (Figure 3-1). At 0.02/My, dynamic pressure in the center of a source rock generating oil is quite low unless the petroleum permeability is exceptionally low. For example, 1 nD source rock with half-thickness of 10 m (66 ft total thickness) develops only 0.032 MPa (4.7 psi). If half-thickness is increased to 100 m (660 ft total thickness), maximum dynamic pressure is 3.2 MPa (467 psi). Permeability on the order of 2.5 pD is required to develop dynamic pressure of 10 MPa (1450 psi) in the center of a 20 m thick source rock.

At the same permeability, thickness, and volumetric generation rate, gas-saturated source rocks develop only about 2% of the excess pressure developed by oil due to gas viscosity about 2% of oil viscosity.

Effects of Volumetric Generation Rate

Effects of volumetric generation rate on maximum dynamic pressure in a 0.1 nD source rock are shown on Figure 3-2. The increase in maximum dynamic pressure is linear with volumetric generation rate. For example, generation rate of 0.02/My and 0.1 nD gives a dynamic excess pressure of about 8 MPa (1160 psi) with 50 m half-thickness (330 ft thick). Volumetric generation rate 4 times higher (0.08/My) gives a dynamic excess pressure of about 32 MPa (4660 psi). Most source rocks have lower volumetric generation rates than 0.02/My, and such high generation rates persist for a short fraction of total generation (Figure 2-5, sheet 2).

Combined Effects

Figure 3-3 shows the combined effects of permeability and volumetric generation rate on maximum dynamic pressure for a source rock with a half-thickness of 20 m (total thickness of 40 m or 131 ft). Excess pressure increases as permeability decreases and generation rate increases. The red rectangle shows the range of generation rates and permeability of most source rocks. Source rocks 40 m and less thick are unlikely to develop significant dynamic excess pressures.

Low dynamic pressure is further indicated by results for typical source rocks (Figures 3-4 and 3-5). Literature and proprietary properties of major source rocks near their depocenters (Figure 3-4) were used to calculate dynamic pressure in the centers of these source rocks at peak oil generation (Figure 3-5). Most source rocks developed low dynamic pressure during peak oil generation, less than 1 MPa (145 psi). Examples with high calculated dynamic pressure have a combination of low permeability, great thickness, and high generation rate.

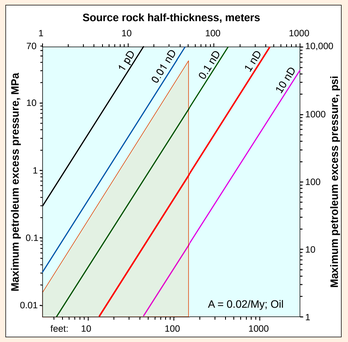

Figure 3-1. Excess pressure in the center of a source rock as a function of permeability and source-rock half-thickness, assuming a generation rate of 0.02/My and viscosity of 1 cp (oil). Shaded area includes range of most source-rock permeability for half-thicknesses up to 50 m (164 ft). High excess pressure requires low permeability (< 0.1 nD) and great thickness.

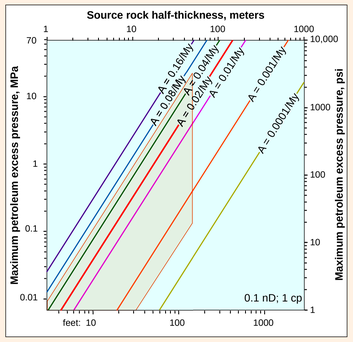

Figure 3-2. Excess pressure in the center of a source rock as a function of volumetric generation rate and source-rock half-thickness, assuming 0.1 nD permeability and 1 cp viscosity (oil). Shaded area is range of generation rates and half-thicknesses up to 50 m (164 ft) characteristic of most source rocks. High excess pressure requires high generation rates and great thickness.

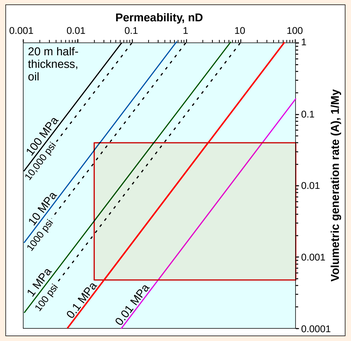

Figure 3-3. Excess pressure in the center of a source rock 40 m (131 ft) thick as a function of permeability and volumetric generation rate. Viscosity of 1 cp (oil) is assumed. Red rectangle includes volumetric generation rates and permeabilities of most source rocks. Most source rocks do not generate significant dynamic pressures.

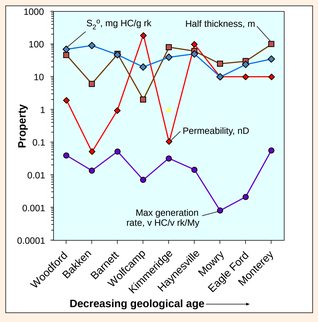

Figure 3-4. Typical properties of major source rocks in areas close to their depocenter. Generation rates are maximum generation rates, and thicknesses are source-facies thickness, not formation thickness. These properties are used to calculate expected dynamic pressure. Data from many sources.

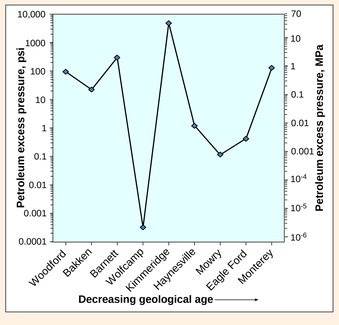

Figure 3-5. Dynamic pressure estimated from source properties shown on Figure 3-4. Most source rocks develop less than 1 MPa (145 psi) dynamic pressure during peak generation. The highest dynamic pressure (Kimmeridge) is caused by low permeability combined with high generation rate and thickness.

Source of Dynamic Pressure

Pressure in source rocks that drives expulsion can arise from two processes: volume changes in the kerogen-oil system and compaction due to overburden weight.

Kerogen - Petroleum Volume Changes

Kerogen volume decreases due to loss of kerogen mass by generation and increasing density as its hydrogen content decreases. If the bulk rock is assumed to neither compact nor expand, the petroleum volume that is expelled is the volume of generated petroleum which exceeds the volume of porosity created by kerogen shrinkage during generation. Where expulsion of this fluid is retarded by rock flow resistance, kerogen volume change generates excess pressure.

Figure 3-6 shows volume changes as a function of transformation for kerogen-petroleum systems with initial hydrogen index of 300 and 700 mg HC/g rk. More petroleum volume is generated than porosity is created by kerogen shrinkage. Part of the petroleum volume fills the kerogen porosity (green) and the rest is expelled (yellow), assuming no compaction. Higher HI^o creates more kerogen porosity. Upon complete transformation, kerogen with 300 HI^o develops about 50% porosity in kerogen whereas kerogen with 700 HI^o develops about 80% porosity in kerogen. Porosity created by kerogen shrinkage in rich source rocks can easily exceed total porosity reported for these source rocks. Porosity from kerogen shrinkage increases with transformation and S_2^o (Figure 3-7). Figured porosity is total porosity in the rock, not porosity in the kerogen.

The expulsion efficiency calculated from kerogen shrinkage in the oil window (assuming no inorganic porosity) is relatively low (<50%, Figure 3-8). Expulsion efficiency calculated from kerogen volume change is much less than that calculated from mass balance in rich source rocks (Figure 1-1, Sheet 1). If petroleum-saturated inorganic porosity is present, expulsion efficiency is even lower than that calculated here. Expulsion efficiency decreases as HI^o increases, because high-hydrogen kerogen shrinks more and thus creates more porosity which retains more petroleum in the source rock. The low expulsion efficiency and opposite trend of expulsion with initial HI predicted from kerogen volume changes indicates that kerogen-petroleum volume change is not responsible for the pressure driving expulsion.

Compaction Equilibrium

Fine-grained, porous rocks exposed to an effective stress compact until grain contacts within the rock support the overburden weight, at which point, compaction stops (Osborne and Swarbrick 1997). The result is an apparent equilibrium between porosity and effective stress referred to as "equilibrium compaction." If porosity in a source rock increases by kerogen shrinkage, and pore pressure does not increase, porosity is no longer in equilibrium with effective stress, and the source rock compacts until it re-equilibrates with effective stress.

Effective stress decreases as pore pressure increases. If high pore pressures develop during petroleum generation, porosity from kerogen shrinkage is preserved as long as high pore pressure persists. If high pore pressure does not develop, porosity created by kerogen shrinkage is lost as quickly as it is formed. If high pore pressure develops but is then dissipated by expulsion as generation rate decreases, organic porosity is transient: it forms in the oil window and decreases after peak oil generation. As organic porosity compacts and kerogen shrinks, the source rock thins.

Typical depths of petroleum generation are on the order of 3 to 5 km. With an overburden stress gradient of 24 MPa/km and hydrostatic pressure gradient of 10 MPa/km, "normal" effective stress gradient is about 14 MPa/km. At 3 and 5 km, pore pressure must increase by 42 MPa (6000 psi) and 60 MPa (10,100 psi), respectively, to reduce effective stress to zero.

For typical source rock thickness, permeability, and generation rates, the maximum dynamic pressure that would develop in source rocks would be on the order of 10 MPa (1450 psi) or less, with most thin source rocks developing negligible (<1 MPa) dynamic pressure (Figures 3-1 to 3-5). With such low dynamic pressure, pore pressure remains close to hydrostatic, and effective stress remains high. Organic porosity should compact as fast as it forms.

Even where source rocks develop high pore pressures during peak generation, the pore pressure dissipates as volumetric generation rates slow after peak generation (Figure 3-9). Generation rates become infinitesimal when the source rock is exhumed. Dynamic pore pressures dissipate rapidly and organic porosity is compacted during exhumation.

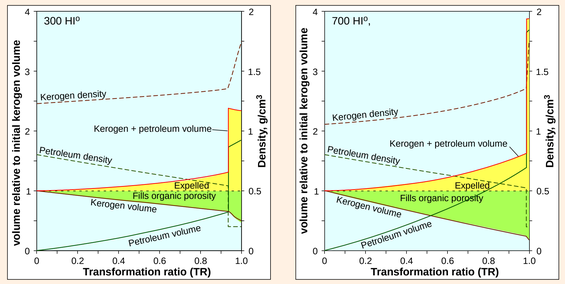

Figure 3-6, Kerogen and petroleum densities (dashed lines) and volume (solid lines) change with transformation. Calculated volumes and expulsion in source rocks with 300 and 700 mg HC/g C initial hydrogen index at left and right, respectively, assuming no porosity compaction. Any excess petroleum volume greater than kerogen shrinkage volume must be expelled (yellow area). Green area is petroleum filling kerogen porosity. Volumes are normalized to initial kerogen volume.

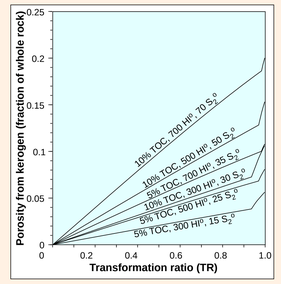

Figure 3-7. Porosity in bulk source rock created by kerogen shrinkage, assuming no compaction or expansion. Porosity roughly increases with S_2^o and TR. Rocks with high S_2^o can create organic porosity approaching 20% of total rock volume. As discussed below, much of this porosity is lost by compaction.

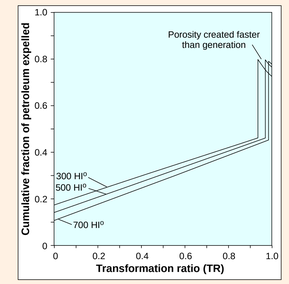

Figure 3-8. Cumulative expulsion efficiency with transformation and initial hydrogen index (HI^o). Oil-window expulsion efficiencies are low, less than 50%, and increase with decreasing HI^o. These results are inconsistent with expulsion efficiencies estimated for actual source rocks; therefore organic porosity compaction must be significant.

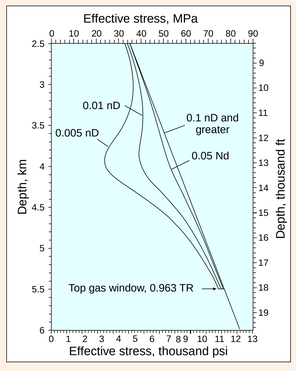

Figure 3-9. Vertical effective stress in center of source rock 50 m thick as a function of depth and permeability for heating rate of 2°C/My and thermal gradient of 30°C/km (67 m/My subsidence rate). Decrease in effective stress is only significant for very low permeability (<0.01 nD). Effective stress rises after peak oil generation due to decreasing dynamic pressure. Any organic porosity preserved by higher excess pressure would be lost. Modeled with Woodford kinetics and properties (440 mg HC/g C HI, 93.5 mg HC/g rk S_2^o). Lower viscosity in gas window offsets increased volumetric generation rate due to lower petroleum density.

Organic Porosity Preservation

The absence or short duration of hard geopressure developing from petroleum generation should result in kerogen compaction as rapidly as it shrinks. This is not the case, because pores 20 nm to 2 microns across are imaged in source-rock kerogen (e.g., Loucks et al. 2012). The reason source rocks do not follow simple effective stress compaction is that the pore types created are different from the pore types lost during compaction and the effective stress-porosity relationship changes as the pore structure changes.

There are several fabrics that will preserve organic porosity: (1) lithification of the silicate framework (orange) around kerogen particles (red) creates a strong framework that will prevent kerogen compaction. Organic porosity (white) is preserved (Figure 3-10A). (2): Isolated rigid grains (yellow) in a ductile matrix (grey) will create a pressure shadow on the sides of the grain that protects some kerogen (red) from compaction (Figure 3-10B). (3): Rigid grains (yellow) in a ductile matrix may touch and form a framework that supports the overburden weight (3-10C). Kerogen (red) in ductile matrix surrounding the framework is protected from overburden weight and porosity is preserved. In the absence of a rigid framework or matrix (Figure 3-4D), kerogen compacts and organic porosity is lost. The rock fabric and strength controls the effective stress-porosity relationship.

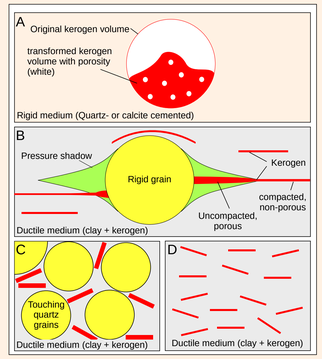

Figure 3-10. Preservation of organic porosity in absence of high pore pressure. (A) Shale matrix has cemented and is no longer ductile. All kerogen shrinkage porosity is preserved. (B) Large, rigid grains in ductile source rock preserve kerogen porosity in pressure shadows on sides of the rigid grain. Part of porosity preserved. (C) Large rigid grains form a framework that bears the overburden weight, kerogen between grains is sheltered from the overburden stress and most organic porosity is preserved. (D) No large, rigid grains and ductile medium: most kerogen porosity compacts as it forms.

Petroleum Expulsion and Formation of Porosity in Kerogen

Brown, Alton A., Consultant, altonabrown@yahoo.com

Comparison to Source Rock Data

Comparison of Storage Models to S_1-Equivalent Volumes

With known rock mineral, kerogen, and petroleum densities, volumes of petroleum stored by different mechanisms (sorption, porosity in organic matter, and inorganic porosity) can be converted to petroleum masses for comparison to stored petroleum mass such as that measured by pyrolysis S_1. Petroleum mass stored by sorption with a fixed mass ratio increases with TOC (red dashed line, Figure 4-1). Petroleum-saturated inorganic porosity storage depends on petroleum and grain density only, not TOC. Combined sorption plus inorganic porosity storage increases with TOC at the same slope as the sorption but with different intercept (the inorganic porosity; black dashed lines, Figure 4-1). Inorganic porosity storage does not change with kerogen density.

In contrast, petroleum stored in organic porosity always has a zero intercept (solid lines, Figure 4-1). Slope with TOC depends on organic porosity and to a lesser extent on kerogen HI (which controls kerogen density). A constant mass-sorption storage can be closely approximated by organic porosity storage. The 100 mg HC/g rk sorption storage in a rock with 430 mg HC/g C hydrogen index is equivalent to storage by 12.55% organic porosity (% porosity in bulk kerogen).

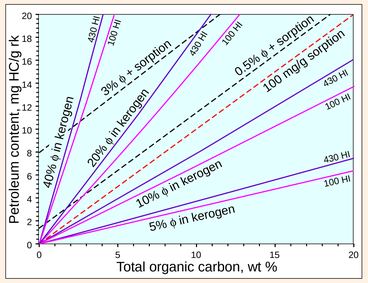

Figure 4-1. Petroleum storage by various mechanisms converted to mass fraction as a function of TOC, % porosity in bulk kerogen, and % petroleum-saturated porosity in rock. Conversion of volumetric quantities stored in kerogen porosity to weight quantities depends on HI. Two HI cases are shown, 430 mg HC/g C (blue lines) and 100 mg HC/g C (red lines). For this example, petroleum and inorganic mineral densities are 0.7 and 2.71 g/cc, respectively.

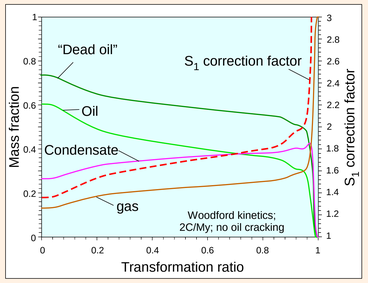

Figure 4-2. Instantaneous petroleum mass fractions during generation from Woodford kerogen. Dead oil is the oil fraction plus half the condensate fraction. The S_1 correction factor (red dashed line) is the inverse of the dead-oil fraction. Kinetics from Di Primio and Horsfield (2006) with heating rate of 2°C/My.

Comparison of Storage Models to S_1 Data

If petroleum in a source rock is stored by a single mechanism, measured petroleum contents should follow a trend against TOC consistent with that mechanism. Where storage mechanisms change with TOC or between source rocks, data trends will cut across modeled trends.

Pyrolysis S_1 data will be used to evaluate storage in three source rocks from three wells in three basins (Table 4-1). Reported S_1 analyses are "dead-oil" concentrations that have to be corrected for loss of volatiles (Cooles et al. 1986). S_1 are corrected by a multiplier which is the inverse of the dead-oil fraction of total generated petroleum mass. The fraction of dead oil in total instantaneous generated petroleum can be estimated from fractions of petroleum products generated in compositional kinetics models. For this study, Woodford compositional kinetics (Di Primio and Horsfield 2006) were used with a heating rate of 2° C/My. The dead oil fraction was assumed to be the weight fraction oil (heptane+) and half the weight fraction of condensate (butane-hexane) products. Over the range of TR of interest, dead oil comprises about 0.6 of the total petroleum (Figure 4-2). S_1 correction factors are listed in Table 4-1.

Corrected S_1 are plotted against TOC and superimposed on trends calculated using 430 HI (Figure 4-3). All data sets show increasing storage with TOC, indicating either significant sorption or porosity storage in kerogen. Eagle Ford data (blue diamonds) have the steepest trend. Barnett data (green squares) have intermediate slope that falls between the 100 mg/g C sorption trend and about 20% organic porosity storage (equivalent to sorption storage plus about 8% organic porosity). Organic porosity storage decreases above about 5% TOC. Bakken data have the lowest slope. At high TOC, Bakken petroleum storage is less than the 100 mg HC/g C sorption storage.

To better evaluate storage in kerogen, the ratio of corrected petroleum content to organic carbon is plotted against TOC (Figure 4-4). Eagle Ford data now more clearly fall on a trend of between 0.5 % and 3 % oil-saturated inorganic porosity with sorption storage (or about 10% organic porosity storage). Barnett data trend falls between 10 and 20% organic porosity in kerogen, possibly mixed with less than 1% petroleum-saturated inorganic porosity (relative to total rock). Lower Bakken data follow a trend of entirely organic porosity where organic porosity decreases with increasing TOC. The Barnett and Bakken trends are consistent with loss of organic porosity by compaction, because increasing kerogen (TOC) content increases ductility and allows more compaction. More organic porosity is preserved at low TOC. Organic porosity in high TOC samples (~ 8 - 10% ϕ in kerogen) are consistent with porosity reported in coals (Gan et al. 1972).

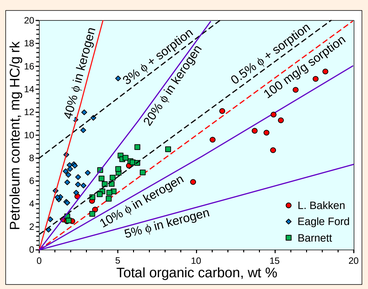

Figure 4-3. Comparison of oil content (corrected S_1) in samples from three source formations to storage by different mechanisms. Trend lines are those for 430 HI shown on Figure 4-1.

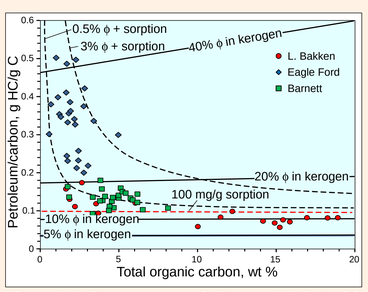

Figure 4-4. Same curves and data as 4-3, but with stored petroleum normalized to organic carbon. Eagle Ford has a mixture of organic porosity (or sorption) with between 0.5% and 3% oil-saturated inorganic porosity. Bakken and Barnett have predominantly organic porosity that decreases with increasing TOC, indicating compaction.

Table 4-1: Example Source Rocks

Formation	Age	Basin	Location	TR	Average hydrogen index (mg HC/g C)	S_1 correction factor	Comments
Lower Bakken	Late Devonian	Williston	Dunn Co. ND, USA	0.59	430	1.8	Data from USGS energy database, well api = 3302500003
Barnett	Mississippian	Fort Worth	Montague Co. TX, USA	0.54	283	1.7	Proprietary data provided by MSRL
Eagle Ford	Cretaceous	South Texas	Dimmit Co. TX, USA	0.79	239	1.7	Newfield Ferguson McKnight #526-1H well; from Romero (2014)

Discussion

Expulsion Pressure

Based on analytical models, maximum pressure in a source rock resulting from petroleum generation (dynamic pressure) is a relatively simple function of petroleum mobility, source-rock thickness, and volumetric generation rate. Based on reasonable values from the literature, dynamic pressures on the order of a few hundred psi (a few MPa) or less are sufficient to expel petroleum at a rate equal to generation in all but the thickest, lowest-permeability source rocks. Many thin source rocks require only a few psi.

High pressures can develop in source rocks, but not from generation. Where fluids at the edge of the source are geopressured by any mechanism, fluid pressure in the source rock is a sum of the dynamic pressure plus geopressure.

If fractures initiate from dynamic pressure plus geopressure in surrounding strata, fractures are more likely to initiate in the middle of source beds (where dynamic pressures are highest) than at tops of beds. Petroleum generation from rich source rocks also causes significant kerogen shrinkage that will cause compaction and fracturing as the kerogen volume shrinks.

Porosity and Expulsion Efficiency

Where kerogen and petroleum density are well constrained, storage mechanisms in source rocks can also be constrained. Both sorption and organic porosity petroleum storage are proportional to TOC or kerogen volume. Such a correlation is evident in most source rocks. In rocks with high TOC, organic porosity (or sorption) storage decreases as TOC increases. This trend is consistent with reduction of organic porosity with increasing TOC. The most likely model for this behavior is compaction of organic porosity. If these Bakken data are representative, the high TOC samples have less petroleum storage than predicted by the commonly assumed 100 mg/g C sorption storage model. Storage by sorption may still be active, but sorption concepts start to merge with porosity storage in submicroporous kerogen where sorption causes swelling. Storage by organic porosity and sorption are both functions of organic matter content in rocks and can operationally be used interchangeably.

Conclusions

Analytical modeling of homogeneous source rock generation demonstrates that excess pressure in source rocks due to generation and expulsion ("dynamic pressure") develop an hyperbolic distribution with highest pressure in the center of the source. This maximum dynamic pressure is dependent only on the mobility (permeability/viscosity), volumetric generation rate, and source-rock thickness. Due to low oil compressibility, pressures equilibrate geologically rapidly, and dynamic pressure can be evaluated by a series of steady models that capture pressure variations as the source rock matures. Pressures scale to the maximum pressure in the center of the bed. This excess pressure is proportional to the volumetric generation rate and source rock half-thickness squared and is inversely proportional to the petroleum mobility.

The maximum excess pressure in an actively generating source rock is relatively low, given realistic volumetric generation rate, source-rock thickness, and source-rock permeability. Hard geopressure is unlikely to develop due to petroleum generation alone. Only exceptionally thick source rocks with permeability less than 0.01 nD and rapid generation rates are likely to develop sufficient geopressure for natural hydraulic fracturing.

The pressure that does develop in source rocks could be due to volume changes in the kerogen-petroleum system or to compaction. Kerogen porosity volumes and expulsion efficiency trends indicate that compaction in response to the overburden weight is the main source of pressure driving expulsion. If the rock compacts, part or all of the porosity generated by kerogen shrinkage during generation may be lost. Where rocks develop a rigid framework and kerogen volume is relatively low, organic porosity is more likely to be preserved. Where kerogen is abundant in the source, the framework appears to be too weak to preserve all kerogen porosity, and organic porosity is lost. Paradoxically, rocks with the highest TOC are likely to have the lowest storage because these rocks are the most susceptible to compaction due to their higher ductility.

References

Aguilera, R., 2016, Shale gas reservoirs: Theoretical, practical and research issues: Petroleum Research, v. 1, p. 10-26.

Brown, A. A., 2002, Petroleum Charge Analysis of the Southern San Joaquin Basin, California: Implications for Future Exploration: 2002 AAPG National Meeting, March 2002.

Byrnes, A. P, S. Zhang, L. Canter, M. D. Sonnenfeld, 2018, Two-phase and three-phase relative permeability of unconventional Niobrara chalk using integrated core and 3D image rock physics: Denver Well logging society presentation in Jan 2018, downloaded from http://dwls.spwla.org/2018-01-16%20DWLS%20 on 25 April 2019.

Carslaw, H. S. and J. C. Jaeger, 1959, Conduction of heat in solids, 2d. ed.: Clarendon Press, Oxford, 510 p.

Cooles, G. P., A. Mackenzie, and T. M. Quigley, 1986, Calculation of petroleum masses generated and expelled from source rocks: Organic geochemistry, v. 10, no. 1-3, p. 235-245.

Di Primio, R. and Horsfield, B., 2006, From petroleum-type organofacies to hydrocarbon phase prediction: AAPG bulletin, v. 90, no. 7, p. 1031-1058.

Eslinger, E. and R. V. Everett, 2009, Petrophysics in generic gas shales with examples from the Haynesville: Haynesville shale gas technology symposium, Society of Petroleum Engineers – Dallas Section, September 15, 2009.

Franklin, R. E., 1948, A note on the true density, chemical composition, and structure of coals and carbonized coals: Fuel, 1948, v. 27, p. 46–49.

Gan, H., S. P. Nandi, and P. L. Walker Jr., 1972, Nature of the porosity in American coals. Fuel, v. 51, no. 4, p. 272-277.

Gorshkov, A. M., L. K. Kudryashova, and O. S. Lee-Van-Khe, 2016, Petrophysical rock properties of the Bazhenov Formation of the South-Eastern part of Kaymysovsky Vault (Tomsk Region): IOP Conference Series: Earth and Environmental Science, v. 43, p. 012010. Downloaded from https://iopscience.iop.org/article/10.1088/1755-1315/43/1/012010/pdf on 25 April 2019.

Han, Z., M. A. Kruge, J. C. Crelling, and B. A. Stankiewicz, 1995, Organic geochemical characterization of the density fractions of a Permian torbanite: Organic geochemistry, v. 22, No. 1, p. 39-50.

Loucks, R. G., R. M. Reed, S. Ruppel, and U. Hammes, 2012, Spectrum of pore types and networks in mudrocks and a descriptive classification for matrix-related mudrock pores: AAPG bulletin, v. 96, no. 6, p. 1071-1098.

Mackenzie, A. S., I. Price, D. Leythaeuser, P. Muller, M. Radke, and R. G. Schaefer, 1987, The expulsion of petroleum from Kimmeridge Clay source-rocks in the area of the Brae oilfield, UK continental shelf: Petroleum geology of north west Europe, v. 2, p. 865-877.

Matthews, C. S. and D. G. Russell, 1967, Pressure buildup and flow tests in wells: H. L. Doherty series, Monograph 1, Society of Petroleum Engineers, Richardson, TX, 167 p.

Milliken, K. L., W. L. Esch, R. M. Reed, and T-W. Zhang, 2012, Grain assemblages and strong diagenetic overprinting in siliceous mudrocks, Barnett Shale (Mississippian), Fort Worth Basin, Texas: AAPG Bulletin, v. 96, no. 8, p. 1553-1578.

Nip, M., J. W. De Leeuw, P. A. Schenck, W. Windig, H. L. C. Meuzelaar and J. C. Crelling, 1989, A flash pyrolysis and petrographic study of cutinite from the Indiana paper coal: Geochimica et Cosmochimica Acta, v. 53, no. 3, p. 671-683.

Okiongbo, K. S, 2011, Bulk volume reduction of the Kimmeridge Clay Formation, North Sea (UK) due to compaction, petroleum generation, and expulsion: Research Journal of Applied Sciences, Engineering, and Technology, v 3, no. 2, p. 132-139.

Okiongbo, K. S., A. C. Aplin, and S. R. Larter, 2005, Changes in type II kerogen density as a function of maturity: Evidence from the Kimmeridge Clay Formation: Energy & fuels, v. 19, no. 6, p. 2495-2499.

Osborne, M. J. and R. E. Swarbrick, 1997, Mechanisms for generating overpressure in sedimentary basins: a reevaluation: AAPG bulletin, v. 81, no. 6, p. 1023-1041.

Pepper, A. S. and P. J. Corvi, 1995, Simple kinetic models of petroleum formation. Part III: modelling an open system: Marine and Petroleum Geology, v. 12, no. 4, p. 417-452.

Robl, T. L., D. N. Taulbee, L. S. Barron, and W. C. Jones, 1987, Petrologic chemistry of a Devonian type II kerogen: Energy & fuels, v. 1, no. 6, p. 507-513.

Stolz. D. J., 2014, Reservoir Character of the Avalon Shale (Bone Spring Formation) of the Delaware Basin, West Texas and Southeast New Mexico: Effect of Carbonate-rich Sediment Gravity Flows: MS thesis, University of Kansas, 165 p.

Sweeney, J. J. and A. K. Burnham, 1990, Evaluation of a simple model of vitrinite reflectance based on chemical kinetics: AAPG bulletin, v. 74, no. 10, p. 1559-1570.

Walls, J. D., A. Morcote, T. Hintzman, M. Everts, 2016, Comparative core analysis from a Wolfcamp formation well; a case study: paper SCA2016-044, International Symposium of the Society of Core Analysts held in Snow Mass, Colorado, USA, 21-26 August 2016, 6 p.

Walls, J. D. and Sinclair, S.W., 2011. Eagle Ford shale reservoir properties from digital rock physics: First Break, v. 29, no. 6, p. 97-101.

Acknowledgments

I thank Bob Loucks and the University of Texas Austin Bureau of Economic Geology MSRL industrial consortium for permission to use Rock Eval Data. I also thank Mark McCaffrey for review of this poster. This work is an expansion of concepts developed when employed at ARCO Oil and Gas company during 1989.